STEM CELLS AND DEVELOPMENT
Volume 25, Number 7, 2016

DOI: 10.1089/scd.2015.0319

Neurogenic Niche Microglia Undergo Positional Remodeling and Progressive Activation Contributing to Age-Associated Reductions in Neurogenesis

Rene Solano Fonseca,[1,2] Swetha Mahesula,[1] Deana M. Apple,[1,2] Rekha Raghunathan,[3] Allison Dugan,[4] Astrid Cardona,[5] Jason O'Connor,[4] and Erzsebet Kokovay[1,2]

Neural stem cells (NSCs) exist throughout life in the ventricular–subventricular zone (V-SVZ) of the mammalian forebrain. During aging NSC function is diminished through an unclear mechanism. In this study, we establish microglia, the immune cells of the brain, as integral niche cells within the V-SVZ that undergo age-associated repositioning in the V-SVZ. Microglia become activated early before NSC deficits during aging resulting in an antineurogenic microenvironment due to increased inflammatory cytokine secretion. These age-associated changes were not observed in non-neurogenic brain regions, suggesting V-SVZ microglia are specialized. Using a sustained inflammatory model in young adult mice, we induced microglia activation and inflammation that was accompanied by reduced NSC proliferation in the V-SVZ. Furthermore, in vitro studies revealed secreted factors from activated microglia reduced proliferation and neuron production compared to secreted factors from resting microglia. Our results suggest that age-associated chronic inflammation contributes to declines in NSC function within the aging neurogenic niche.

Introduction

Neurogenesis continues throughout life in the mammalian ventricular–subventricular zone (V-SVZ) that lines the lateral wall of the lateral ventricle [1,2] and the subgranular zone of the hippocampal dentate gyrus [3,4]. In this study, we focus on V-SVZ neural stem cells (NSCs), which have distinct regulatory signals, niche organization, developmental origin, and neuronal output from hippocampus-derived NSCs [5–9].

V-SVZ NSCs are astrocyte-like cells that divide slowly to produce rapidly dividing transit-amplifying cells (TACs), which expand the progenitor pool and ultimately produce neuroblast cells. These neuroblasts migrate out of the V-SVZ to the olfactory bulb, where they integrate and differentiate into granule or periglomerular neurons [1,10]. Under certain pathological conditions, V-SVZ NSCs increase proliferation and migrate to the injury site, where they give rise to a limited number of neurons, oligodendrocytes, and astrocytes, which have been shown to contribute to repair [11–15].

During aging, V-SVZ neurogenesis declines rapidly around mid-age [16–18], resulting in olfactory memory deficits [19]. The mechanism for this decline is not clear, however, changes within the NSC niche have been clearly documented. NSCs possess an apical process that protrudes through the ependymal layer, contacting the lateral ventricle. This apical process is capped by the adhesion molecule VCAM1, which anchors NSCs within the niche [20]. When viewed en face, ependymal cells surround clusters of these NSC processes expressing VCAM1 and form germinal units that appear as pinwheels. The number of germinal pinwheels declines during aging and this is accompanied by ependymal cell loss, stenosis of the lateral ventricle, and an overall reduction in V-SVZ germinal area [21].

NSCs also send out a basal process that contacts the vascular plexus on the opposing side of the V-SVZ, where they receive signals important for quiescence, proliferation, and lineage progression [22]. During aging, the vasculature undergoes extensive remodeling with a reduction in density and blood flow [23] and changes in orientation [24]. However, the impact of aging on other cells in the V-SVZ niche and the subsequent effect on NSC function in the aged brain is unknown.

In this study, we investigated the spatiotemporal changes in position and activation state of microglia in the adult V-SVZ niche during aging. Microglia, the innate immune cells of the brain, are distinct from peripheral macrophages developmentally, phenotypically, and have a unique transcriptome [25,26]. Under basal conditions, microglia

Departments of [1]Cellular and Structural Biology, [4]Pharmacology, University of Texas Health Science Center at San Antonio, San Antonio, Texas.
[2]Barshop Institute for Longevity and Aging Studies, San Antonio, Texas.
[3]Molecular and Translational Medicine, Boston University, Boston, Massachusetts.
[5]Department of Biology, University of Texas at San Antonio, San Antonio, Texas.

exhibit a characteristic ramified morphology with processes continuously in motion surveying the surrounding environment [27].

Following injury or infection, microglia become activated, leading to morphological changes, proliferation, and secretion of proinflammatory cytokines [28,29]. During aging, microglia become hypervigilant, expressing increased levels of proinflammatory cytokines and overreact to normal subthreshold immune challenges, leading to an exaggerated immune response deleterious to brain function [30–32]. In the hippocampus, microglia have been shown to be both positive and negative regulators of neurogenesis depending on activation state [33–37]. In addition, during the early postnatal period, microglia in the V-SVZ are proneurogenic in vitro and in vivo [38]. However, little is known about their role in adult V-SVZ neurogenesis during tissue homeostasis or aging.

Although, not typically included as one of the principal cellular components of the adult V-SVZ neurogenic niche, we found that microglia are located throughout the V-SVZ and are associated with germinal pinwheels, transit-amplifying cells, neuroblasts, and the vascular plexus. The relationship of microglia to other niche cells becomes drastically altered during aging. Microglia in the V-SVZ are unique in their activation state and became progressively activated during aging, and this is not seen in non-neurogenic regions of the brain. This progressive activation produced a proinflammatory microenvironment in the V-SVZ niche, which was accompanied by infiltrating peripheral monocytes. Interestingly, we found that resting microglia are proneurogenic in an in vitro model. However, activation of microglia in vivo and in vitro reduced proliferation and neuronal output.

Materials and Methods

Mice

For microglia and NSC cultures, Swiss Webster mice (aged 2 months) were bred at the UTHSCSA vivarium. For aging studies, C57/Bl6 mice aged 2–4 (young adult), 6–8 (adult), 10–14 (mid-aged), and 15–24 (aged) months were obtained from the National Institute of Aging. All animals were provided free access to water and standard rodent chow ad libitum. All mouse studies were approved by the University of Texas Health Science Center at San Antonio Institutional Animal Care and Use Committee and performed in accordance with institutional and federal guidelines.

Immunohistochemistry

For wholemount immunohistochemistry, brains were isolated, halved, the cortex and septum removed to reveal the SVZ, and fixed in 4% paraformaldehyde overnight at 4°C. SVZ wholemounts were then microdissected and permeabilized with 2% PBST. Cell cultures were fixed in 4% PFA for 15 min at RT and permeabilized with 0.1% PBST. Before primary antibody incubation, the tissue was incubated in blocking solution containing 10% normal donkey serum in the appropriate PBST concentration overnight at 4°C. Incubation in primary antibodies was performed in blocking solution overnight at 4°C. The primary antibodies used were MASH1 (1:200; Cat. No. 556604; BD, Franklin Lakes, NJ), doublecortin (1:200; Cat. No. SCB066; Santa Cruz Biotechnology, Dallas, TX), Iba1 (1:200; Cat. No. 019-19741; Wako Chemicals, Richmond, VA), CD68 (1:250; Cat. No. MCA1957; AbD Serotec, Raleigh, NC), VCAM1 (1:50; Cat. No. 550547; BD), β-catenin (1:50; Cat. No. 610154; BD), CD31 (1:100; Cat. No. 550274; BD), βIII-Tubulin (1:500; Cat. No. MMS-435P-250; Covance, Austin, TX), and bromodeoxyuridine (BrdU; 1:250; Cat. No. NB500-169; Littleton, CO). Species-specific secondary antibodies (Jackson ImmunoResearch, West Grove, PA) were used at a concentration of 1:250.

RNA extraction and quantitative real time polymerase chain reaction

Total RNA was extracted from SVZ wholemounts using the mirVana miRNA Isolation Kit (Ambion, Life technologies, Waltham, MA) according to the manufacturer's instructions. cDNA was synthesized from 1 μg of total RNA using High-Capacity cDNA Reverse Transcription (Applied Biosystems, Life technologies). Quantitative polymerase chain reaction (PCR) was performed using a 7,500 Real-Time PCR System Thermal Cycler (Applied Biosystems) by SYBR® Green PCR master mix (Applied Biosystems). Glyceraldehyde 3-phosphate dehydrogenase was used as endogenous control. Negative control qRT-PCR were carried out under the same conditions in the absence of cDNA. Reactions were performed in triplicate. Quantification was analyzed by the ΔΔCt method as described [39]. Primers used were: IL-6 (Forward = CAACGATGATGCACTTGCAGA; Reverse = GGTACTC CAGAAGACCAGAGG); IL-1β (Forward = GGAGAACC AAGCAACGACAAAATA; Reverse = TGGGGAACTCTG CAGACTCAAAC); TNFα (Forward = GGAACACGTCG TGGGATAATG; Reverse = GGCAGACTTTGGATGCTT CTT).

BCG inoculation

Male C57/Bl6 mice (2-month-old) were inoculated with *Mycobacterium bovis*, Bacillus Calmette–Guérin (BCG) as previously described [40]. Briefly, mice received 1.5×10^6 colony-forming units intraperitoneally in a volume of 0.5 mL. Control animals received 0.5 mL of sterile saline. Dispersed BCG stocks, derived from TheraCys, BCG Connaught strain (Lot#C3705AA; Sanofi Pasteur, Ontario, Canada), were prepared immediately before injection by 30 s vortex, 10 min warm water bath sonication, and six passages through a 25-gauge needle.

EdU labeling and staining in wholemounts

Mice were injected with EdU intraperitoneally (200 μg/mouse) 2 h before they were sacrificed and the brains removed. Brains were then halved and the ventricles were exposed for overnight fixing in 4% PFA at 4°C. EdU staining proceeded according to the manufacturer's instructions (Click-it EdU Imaging Kit; Life Technologies).

BrdU labeling and staining in sections

Mice were injected with BrdU (10 ng/mL solution) intraperitoneally (50 mg/kg) 2 h before they were sacrificed and perfused with cold 1× phosphate buffered saline (PBS) followed

by 4% paraformaldehyde. 30 μm serial coronal brain sections were cryosectioned and collected as floating sections in 1× PBS. Every sixth section was permeabilized in PBS with 0.3% Triton for 45 min at room temperature. The sections were then incubated in 2N HCl at 37°C for 1 h followed by two 5 min washes in borate buffer and then immunostained. The number of BrdU cells per section was counted using a fluorescent microscope by two separate individuals, and numbers per section were averaged between both counts.

NSC cultures

V-SVZs of young adult mice (2-month-old) were microdissected and minced to 1 mm^2 pieces in adult hibernation medium (30 mM potassium chloride, 5 mM sodium hydroxide, 5 mM anhydrous monosodium phosphate, 0.5 mM magnesium chloride hexahydrate, 20 mM sodium pyruvate, 5.5 mM glucose, and 200 mM sorbitol). Dissociation proceeded in 100 U of papain in DMEM/F12 at 37°C for 45 min on a shaker and gently triturated. Cells were washed three times with DMEM/F12 and centrifugation at 400 *g* for 10 min. After centrifugation, cells were resuspended in 1 mL serum-free medium and counted. Adherent cultures were obtained by plating cells in 24-well plates coated with poly-ornithine/laminin at 50,000 cells per well in NSC serum-free medium (high glucose DMEM supplemented with 0.1 mM sodium pyruvate, 1× GlutaMAX [Gibco, Thermo Fisher Scientific, Waltham, MA], N-2 [Gibco], B27 [Life Technologies], and 10 ng/mL bFGF [PeproTech, Rocky Hill, NJ]).

Microglia isolation, resting microglia (M0), and activated microglia (M1) cultures

Swiss Webster mice (2–4 month old) were perfused with cold 1× HBSS (without Mg^{2+}/Ca^{2+}). Whole brains were harvested and minced to 1 mm^2 pieces and dissociated with the Miltenyi (San Diego, CA) Brain Dissociation Kit following the manufacturer's instructions. Following dissociation, myelin was removed through a 22% Percoll gradient. After myelin removal, the cells were incubated in CD11b-APC conjugated antibodies for 30 min at 4°C and FACS sorted. Microglia were plated in six-well plates coated with poly-ornithine/laminin at 300,000 cells per well in microglia serum media (DMEMF/12 with 10% fetal bovine serum, 1× GlutaMAX [Gibco], and 10 ng/mL GM-CSF) and expanded for 5 days. To generate resting microglia (M0), the adult primary microglia were cultured in microglia medium supplemented with 10 ng/mL mouse recombinant carrier-free MCSF and 50 ng/mL human recombinant TGFβ1 for 5 days [26]. To generate activated microglia (M1), the adult primary microglia were cultured in microglia medium supplemented with 5 ng/mL mouse recombinant carrier-free MCSF for 5 days, 20 ng/mL of IFNγ for 1 h, and 1 μg/mL lipopolysaccharide (LPS) for 2 days [41].

Conditioned medium experiments

Microglia were cultured in microglia medium until confluent and then switched to NSC serum-free medium. After 24 h, media were collected. Likewise, NSCs were expanded in NSC serum-free medium until confluent before media were collected. All conditioned media were filtered through 0.2-μm syringe filters at the time of collection. Approximately 48 h after NSCs were plated in 24-well dishes at 50,000 cells per well, cultures were switched to either microglia conditioned media, or control NSC conditioned media. All media were supplemented with 10 ng/mL bFGF. Media were changed every 2 days. After 4 days in culture, cells were fixed with 4% paraformaldehyde.

Data quantification

CD68 and Iba1 reactivity in the V-SVZ was quantified using the ''Analyze particles'' function of ImageJ on wholemounts. Microglia distance from blood vessels was quantified using the statistics function of Imaris on 3-dimensional renderings from V-SVZ wholemounts. CD68 and Iba1 reactivity in the striatum was quantified using the ''Analyze particles'' function of ImageJ on brain sections. Microglia clustering was quantified using the ''Events'' function in the ZEN software (Zeiss, Jena, Germany), where a cluster of microglia was assessed when 2 or more Iba1-positive cell bodies were closer than 5 μm or making contact with each other. Infiltrating monocytes in the Cx3cr1-GFP/Ccr2-RFP mice and EdU+ cells in the BCG-injected mice were quantified using the ''Events'' function in the ZEN software (Zeiss) on V-SVZ wholemounts. Cell culture experiments were quantified from 10 random fields of view obtained with a 20× objective in a Zeiss Axio Observer.D1 and using the ''Events'' function in the ZEN software (Zeiss). BrdU-positive cells in the V-SVZ were quantified by eye with a Zeiss Axio Observer.D1. Brain sections were analyzed from 15 μm thick Z-stacks. V-SVZ wholemounts were analyzed from 25 μm thick Z-stacks (10 Z-stacks per wholemounts). Confocal images were obtained with a Zeiss LSM 710 confocal microscope.

Statistical analysis

ANOVA and student's *t*-tests were used to analyze the data on GraphPad Prism 5 Software. All data are expressed as mean ± standard error of mean.

Results

Microglia association with niche cells changes during aging

To determine the spatial and temporal changes in microglia's relationship to other niche cells, we performed immunohistochemistry on the adult V-SVZ wholemounts, which preserves the 3-dimensional cytoarchitecture of the entire V-SVZ niche [2,20,42,43] combined with confocal microscopy and 3-dimensional image analysis using Imaris software. We used antibodies generated against ionized calcium binding adaptor molecule 1 (Iba1) to label microglia.

In young adult mice (2 months old), we found that microglia had a typical ramified morphology and were evenly distributed throughout the V-SVZ with very little to no overlap between their processes. Doublecortin immunostaining revealed that microglia processes were closely associated with migrating chains of neuroblasts (Fig. 1A), MASH1+ TACs (Fig. 1B) and GFAP+ NSCs, and niche astrocytes (Fig. 1C). In 12-month-old mice, the numbers of neuroblasts and TACs were drastically reduced, however, we still observed microglia processes associated with neuroblasts, TACs, and GFAP+ cells (Fig. 1).

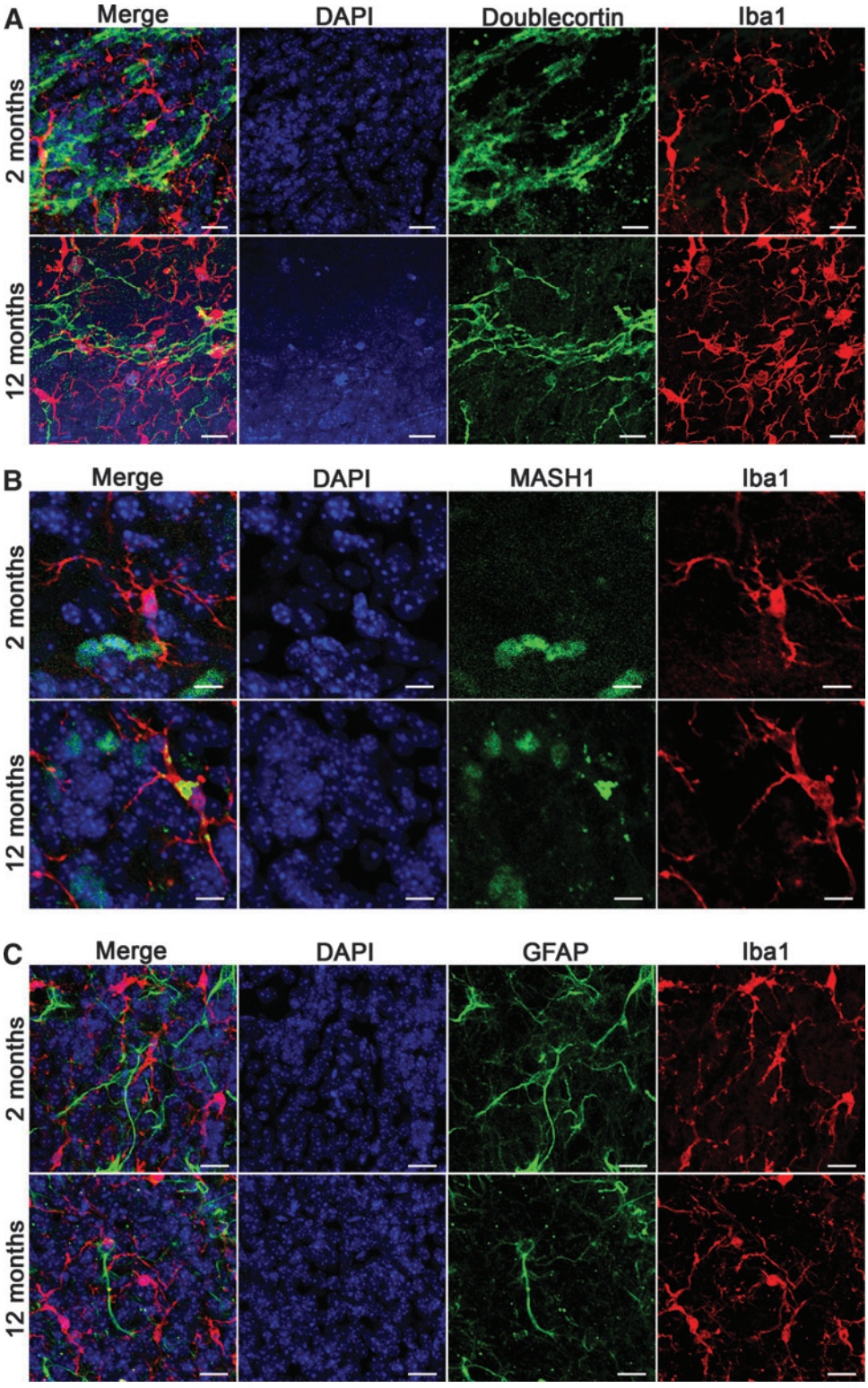

FIG. 1. Relation of microglia to niche cells of the ventricular–subventricular zone (V-SVZ) in 2- and 12-month-old mice. **(A)** Confocal projection images of neuroblasts (dcx) and microglia (Iba1) in 2- and 12-month-old mice. Scale bar: 20 μm. **(B)** Confocal projection images of transient amplifying cells (MASH1) and microglia (Iba1) and in 2- and 12-month-old mice. Scale bar: 10 μm. **(C)** Confocal projection images of GFAP-positive cells and microglia (Iba1) in 2- and 12-month-old mice. Scale bar: 20 μm.

The distribution of microglia in the aged V-SVZ differs significantly from the distribution observed in the young adult mouse. While at 2 months of age, microglia appear evenly distributed throughout the niche, at 12 months of age, the uniformity of microglia distribution appeared to deteriorate (Fig. 2A). A trend of increases in microglia clustering was evident between 2, 6, 12, and 24 months (Fig. 2B), where statistical significance was observed between 2 and 24 months (Fig. 2B; 10.00 ± 2.517 vs. 25.50 ± 1.50 Iba1-positive cell clusters per field; $P = 0.0139$) and between 6 and 24 months (Fig. 2B; 12.67 ± 2.728 vs. 25.50 ± 1.50 Iba1-positive cell clusters per field; $P = 0.0139$).

Next, we colabeled microglia and type B NSC end-feet in germinal pinwheels using VCAM1 and β-catenin immunohistochemistry in 2-month-old mice. This revealed that microglia extend processes through the ependymal layer making

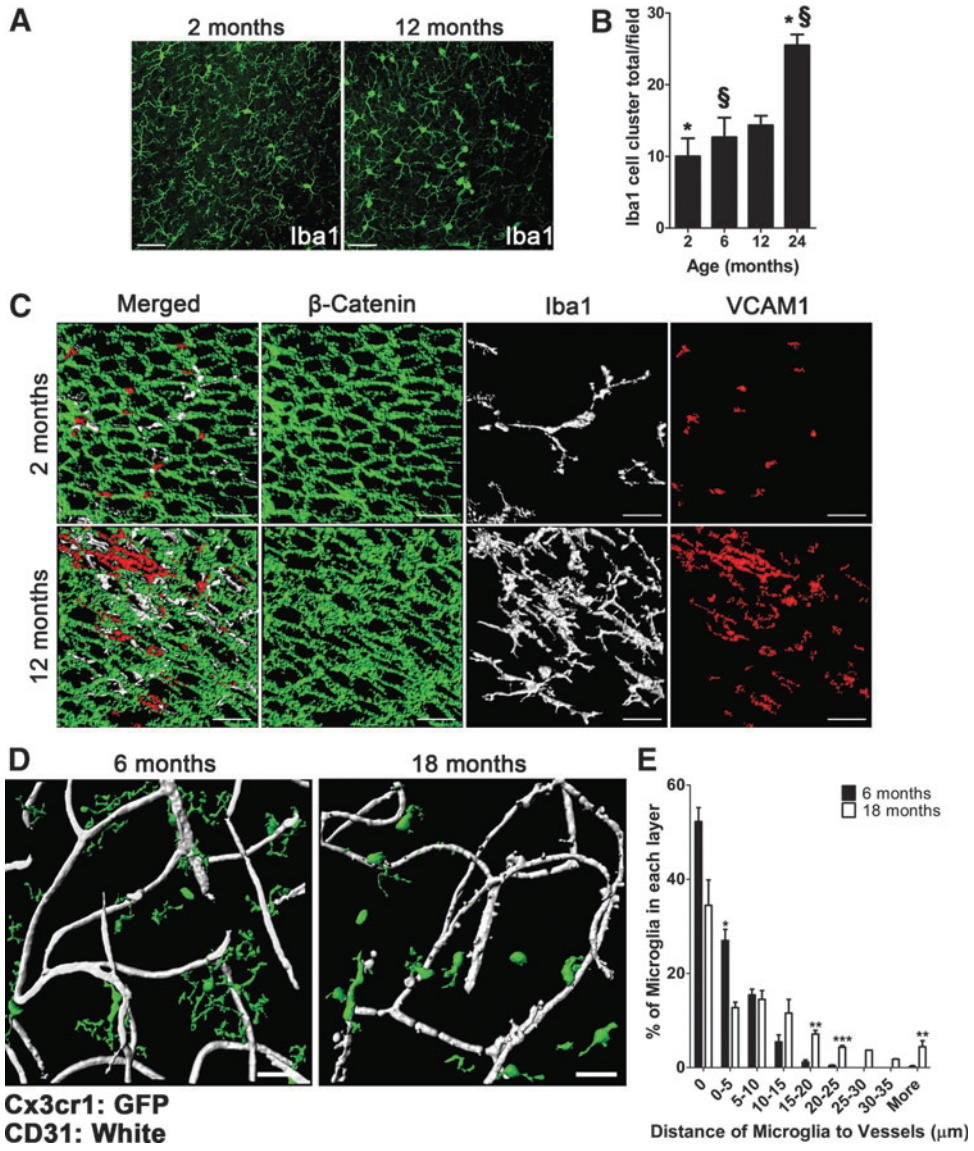

FIG. 2. Age-related changes in microglia distribution and organization in the V-SVZ. **(A)** Low magnification (25×) confocal images of the distribution of microglia in 2- and 12-month-old mice. Scale bar: 50 μm. **(B)** Quantification of microglia clumping in 2-, 6-, 12-, and 24-month-old mice. $n = 3$ per group. Error bars = standard error of mean (SEM). $*,^{\S}P \leq 0.05$. **(C)** Imaris 3-dimensional reconstruction of confocal images of microglia (Iba1) within germinal pinwheels (VCAM1 for neural stem cell [NSC] endfeet and β-catenin for ependymal cell junctions) in 2- and 12-month-old mice. Scale bar: 20 μm. **(D)** Imaris 3-dimensional renderings of GFP-expressing microglia and CD31-labeled vasculature at 6 and 18 months old. Scale bar: 30 μm. **(E)** Quantification of the distance of microglia cell bodies relative to blood vessels in the V-SVZ at 6 ($n = 4$) and 18 ($n = 3$) months. Error bars = SEM. $*P \leq 0.05$; $**P \leq 0.01$; $***P \leq 0.001$.

contact with the lateral ventricle near germinal pinwheels (Fig. 2C). In 12-month-old mice, VCAM1 no longer exhibited a punctate expression in the center of pinwheels suggesting remodeling of germinal pinwheels during aging.

Furthermore, we observed large clusters of hyper-ramified microglia closely associated with the ependymal layer (Fig. 2C). We also observed microglia closely associated with the niche vascular plexus in adult mice (6 months old) with processes making direct contact with blood vessels. By mid-age (12 months old), there was a significant increase in the distance of microglia cell bodies from niche vasculature, which was accompanied by protracted processes and amoeboid morphology (Fig. 2D and E).

Microglia display early and progressive activation in the V-SVZ niche during aging

Before assessing the status of microglia activation during aging, we confirmed the timing of the age-related decline in adult V-SVZ neurogenesis reported by others [16,18,24] by counting the number of BrdU-positive cells following a 2 h pulse in coronal brain sections [20,44] and by quantifying the number of cells labeled with the neuroblast marker doublecortin (Dcx) in V-SVZ wholemounts. Indeed we observed a dramatic and significant decline in V-SVZ proliferation between 6- and 12-month-old mice (Fig. 3A; 145.6 ± 8.010 vs. 31.20 ± 6.492 average BrdU-positive cells per section; $P < 0.0001$) as well as a significant reduction of neuroblasts between 2- and 24-month-old mice (Fig. 3B, C; 38.13 ± 6.501 vs. $9.331\% \pm 1.693\%$ Dcx-labeled cells per field; $P = 0.0052$).

To assess microglia activation status during aging, we used immunohistochemistry against the microglia marker Iba1 and the activated microglia marker, CD68, a glycoprotein that binds to low-density lipoprotein. In young adult mice, microglia had the classic ramified morphology of resting microglia with very little CD68 reactivity. In contrast, by 12 months of age (mid-age), we observed clusters of hyper-ramified microglia that began to highly express CD68. By 24 months of age, clusters of microglia were found throughout the adult V-SVZ niche with high CD68 reactivity and an amoeboid or round morphology, indicative of progressive microglia activation during aging (Fig. 3D).

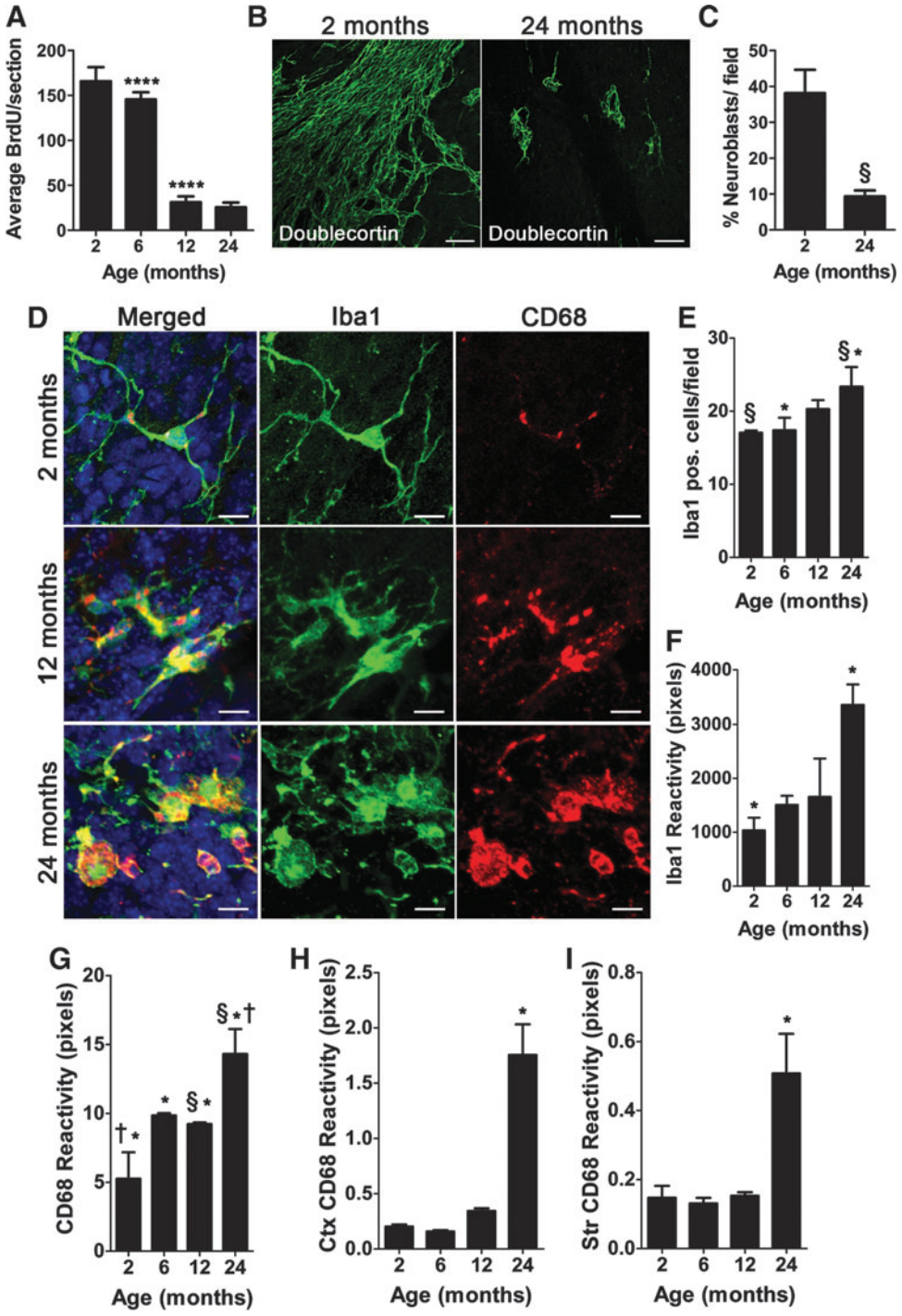

FIG. 3. Early age-related increased microglial activation in the V-SVZ, but not in non-neurogenic brain regions. **(A)** Quantification of proliferating BrdU-positive cells in the V-SVZ. $n=5$ per age group. **(B)** Representative confocal images of doublecortin-labeled V-SVZ wholemounts in 2- and 24-month-old mice. Scale bar: 50 μm. **(C)** Percentage of neuroblasts per field in wholemounts. $n=4$ per group. **(D)** Confocal images from 2- to 12- and 24-month-old mice staining for Iba1 (*green*), CD68 (*red*), and DAPI (*blue*). Scale bar: 10 μm. **(E)** Quantification of the number of Iba1+ cells in 2-, 6-, 12-, and 24-month-old mice in the V-SVZ. **(F)** Total area covered by Iba1+ cells per field assessed with ImageJ in the V-SVZ. **(G)** Size of CD68 reactivity in individual cells assessed with ImageJ. **(H)** CD68 reactivity in the cortex (Ctx) assessed with ImageJ. **(I)** CD68 reactivity in the striatum (Str) assessed with ImageJ $n=3$ per group. Error bars = SEM. $^{*}P\leq 0.05$; $^{\S}P\leq 0.01$; $^{\dagger}P\leq 0.001$; $^{****}P\leq 0.0001$.

Quantification of the number of microglia at 2, 6, 12, and 24 months of age revealed that the numbers of microglia progressively increases with aging, however, this did not reach significance until 24 months of age (Fig. 3E), although patches of the V-SVZ niche appear to have increased microglia number due to increased microglia clustering as described in Figure 2A, and B. Microglia Iba1 expression levels also increased during aging between 2 and 24 months (Fig. 3F; $1{,}034\pm235.1$ vs. $3{,}361\pm380.8$ average total pixels per field; $P=0.0002$). Quantification of CD68 reactivity revealed an early increase in CD68 expression of microglia between 2 and 6 months (Fig. 3G; 5.254 ± 1.109 vs. 9.849 ± 0.0967 average total pixels per field; $P=0.0002$), which was sustained at 12 months (Fig. 3G; 5.254 ± 1.109 vs. 9.224 ± 0.0726 average total pixels per field; $P=0.0002$) before increasing again at 24 months (Fig. 3G; 5.254 ± 1.109 vs. 14.31 ± 1.04 average total pixels per field; $P=0.0002$).

Next, we asked the question, is microglial activation a global brain phenomenon due to aging or unique to the V-SVZ niche? Interestingly, we measured very little change in CD68 reactivity in the cortex and striatum (Fig. 3H, I) until 24

months of age, suggesting that microglia in the adult V-SVZ undergo an early and sustained activation that is not reflected in non-neurogenic areas of the brain.

Microglia undergo well-defined morphological changes that correlate and distinguish their activation state, and we scored and quantified the number of microglia having a ramified (Fig. 4A), hyper-ramified (Fig. 4B), amoeboid (Fig. 4C), or round morphologies (Fig. 4D) using immunohistochemistry to Iba1. The ramified and hyper-ramified microglia correlate with a resting and intermediate activation state, respectively, whereas amoeboid and round microglia are considered to be in higher activation states [45]. Mice of 12 months of age revealed higher number of hyper-ramified microglia as well as amoeboid microglia when compared to 2- and 6-month-old mice. At 24 months of age, most of the microglia were observed to be at higher activation stages (Fig. 4E) with a paucity of microglia with ramified or hyper-ramified morphology.

Since microglia activation is associated with increased inflammation [28,29], the expression of the proinflammatory molecules TNFα, IL-1β, and IL-6 was measured by qRT-PCR from isolated adult V-SVZs (Fig. 4F). An increase in the expression of TNFα (1.0170 ± 0.1054 vs. 1.6 ± 0.1514 relative expression), IL-1β (1.1770 ± 0.4179 vs. 3.9220 ± 0.7605 relative expression), and IL-6 (1.1200 ± 0.3496 vs. 21.2500 ± 11.080 relative expression) was observed in aged mice (15 months) when compared to young adult mice (2–4 months). Interestingly, we observed an increase in IL-6 expression as early as 6 months of age (Fig. 4G; 1.159 ± 0.4345 vs. 4.315 ± 0.8464 relative expression) suggesting some degree of inflammation takes place before deficits in neurogenesis appear between 7 and 12 months of age. Taken together, these results indicate an early and progressive activation of microglia and inflammation in the V-SVZ niche during aging that is not reflected in non-neurogenic regions based on morphological changes and microglial distribution.

Peripheral macrophage/monocytes contribute to the inflammatory response in the V-SVZ

Because we saw an increase in Iba1-positive cells during aging, we assessed the contribution of peripheral macrophages/monocytes into the V-SVZ during aging. To test this, we utilized $Cx3cr1^{+/GFP}CCR2^{+/RFP}$ reporter mice that distinguished peripheral monocytes/macrophages from resident microglia. Microglia in these mice are CX3CR1-GFP^{Hi}/CCR-RFP^{Neg}, whereas inflammatory blood-derived monocytes are CX3CR1-GFP^{lo}/CCR-RFP^{Hi}, making peripheral monocytes distinguishable from microglia based on the presence of RFP expression [25].

In young adult mice (6 months), we found very low numbers of RFP+ cells within the V-SVZ niche, whereas in aged mice (18 months), there was a significant increase in the number of cells displaying a punctuate pattern of RFP expression (Fig. 5A, B; 7.975 ± 0.6574 vs. 27.25 ± 3.830 percent monocytes to total microglia; $P = 0.0032$). Furthermore, in aged mice, high numbers of RFP-expressing cells were present in clusters of microglia with amoeboid and round morphology (Fig. 5A), indicative of their involvement in the inflammatory response in the neurogenic niche.

Sustained systemic inflammation reduces proliferation in young adult mice

Acute inflammation following LPS injection has been shown to result in activation of NSCs resulting in increased proliferation in the V-SVZ [46] suggesting that inflammation per se is not deleterious to neurogenesis. However, we observed chronic inflammation in the V-SVZ in mid-aged to aged mice concomitant with reduced neurogenesis, suggesting that sustained inflammation is deleterious to NSC function. To induce sustained inflammation we inoculated young adult mice with Bacillus Calmette–Guérin, an attenuated form of *Mycobacterium bovis* that induces robust and prolonged inflammation both in brain and the periphery [47]. We assessed proliferation of NSC and the time course of microglia activation at 1 and 2 weeks following inoculation.

At 1 week we observed a significant rise in microglial CD68 expression when compared to PBS-injected control mice, but only a trend in reduced proliferation (data not shown). Two weeks following BCG injection, we observed a significant increase in CD68 immunoreactivity (Fig. 6A, B; $1{,}674 \pm 101.2$ vs. $3{,}430 \pm 279.2$ average volume per cell; $P = 0.0056$) and cell proliferation was significantly attenuated in mice inoculated with BCG when compared to vehicle-injected mice (Fig. 6A, C; 697.4 ± 17.17 vs. $1{,}012 \pm 73.92$ average EdU-positive cells; $P = 0.0467$).

Scoring microglia for morphological stages of activation, we observed an increase in microglia with activated morphologies in mice that received BCG compared with saline-injected controls (Fig. 6D). However, mice that received a saline injection had a modest increase in activated microglia with activated morphologies that we observed in uninjected mice (Fig. 4E) indicating that the stress of IP injections alone can cause an immune response as has been observed by others [48,49]. Overall, these results suggest that sustained microglia activation and inflammation in young adult mice (2 months old) significantly reduces neurogenesis in the V-SVZ.

Activated microglia reduce neurogenesis, whereas resting microglia increase neurogenesis and proliferation

Next, we utilized an in vitro system to test the influence of resting microglia versus activated microglia on adult V-SVZ NSC proliferation and neurogenesis. To do this, we cultured primary V-SVZ NSC in the presence of conditioned media from young adult microglia induced either to an activated state (M1) or a resting state (M0) using IFNγ/LPS or TGFβ, respectively [26,41]. We chose this regimen because it has been shown to resemble the phenotype of acutely isolated resting microglia and activated microglia [26].

We found a significant reduction in proliferation as measured by EdU uptake in NSCs cultured in conditioned medium from activated microglia (M1) compared to NSCs cultured in conditioned medium from resting microglia (M0) (Fig. 7A, B; 11.64 ± 0.18 vs. 3.883 ± 1.301 percent EdU-positive cells per field; $P = 0.0192$). However, a reduction in proliferation was not seen compared to NSCs cultured in the presence of control medium. We also found that, M1 conditioned medium induced a significant reduction in neuron production, as measured by βIII-tubulin expression, when

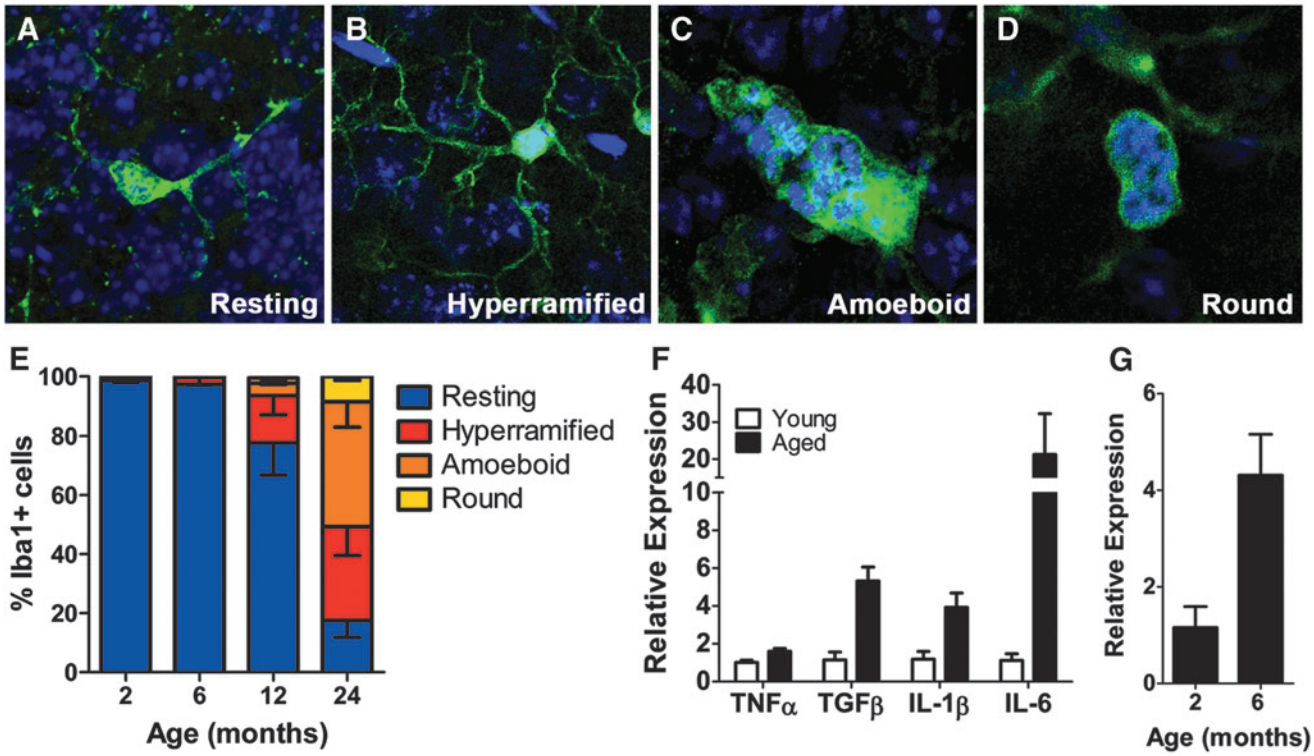

FIG. 4. Inflammation-associated morphological stages of microglia activation and proinflammatory cytokine expression in the V-SVZ of aged mice. **(A–D)** Resting, hyper-ramified, amoeboid, and round morphologies of microglia activation. Iba1 (*green*), DAPI (*blue*). Scale bar: 10 μm for **(A, B)**; Scale bar: 5 μm for **(C, D)**. **(E)** Quantification of the different stages of microglia activation (as in **A–D)** in the V-SVZ wholemounts of 2-, 6-, 12-, and 24-month-old mice ($n = 3$ per group). **(F)**. Relative expression of the proinflammatory cytokines TNFα, IL-1β, and IL-6 as measured by quantitative real time-polymerase chain reaction (qRT-PCR) from the V-SVZ of young adult (2–4 months) and aged (12–15 months) mice ($n = 4$ per group). **(G)** Relative expression of IL-6 as measured by qRT-PCR from the V-SVZ of 2 ($n = 3$) and 6 ($n = 2$)-month-old mice. Error bars = SEM.

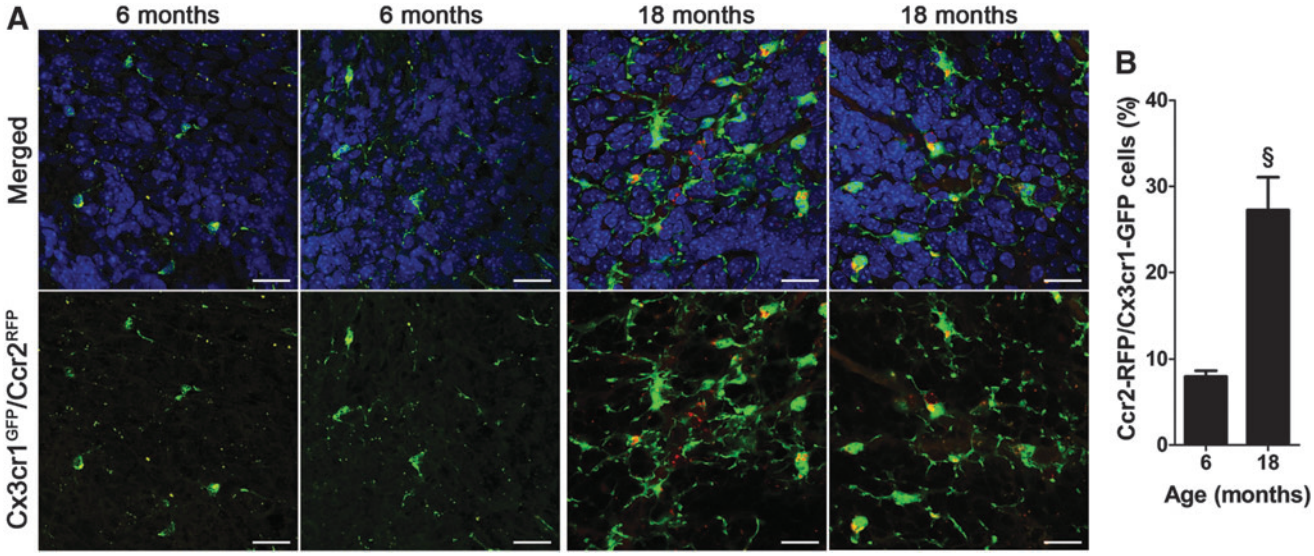

FIG. 5. Increasing infiltration of peripheral macrophages/monocytes in the aging V-SVZ. **(A)** Representative images of GFP expressing microglia and RFP expressing monocytes in V-SVZ wholemounts at 6 ($n = 4$) and 18 ($n = 5$) months. Scale bar: 20 μm. **(B)** Quantification of peripheral infiltrating macrophages/monocytes in relation to total GFP-expressing resident microglia. $^{\S}P \leq 0.01$. Error bars = SEM.

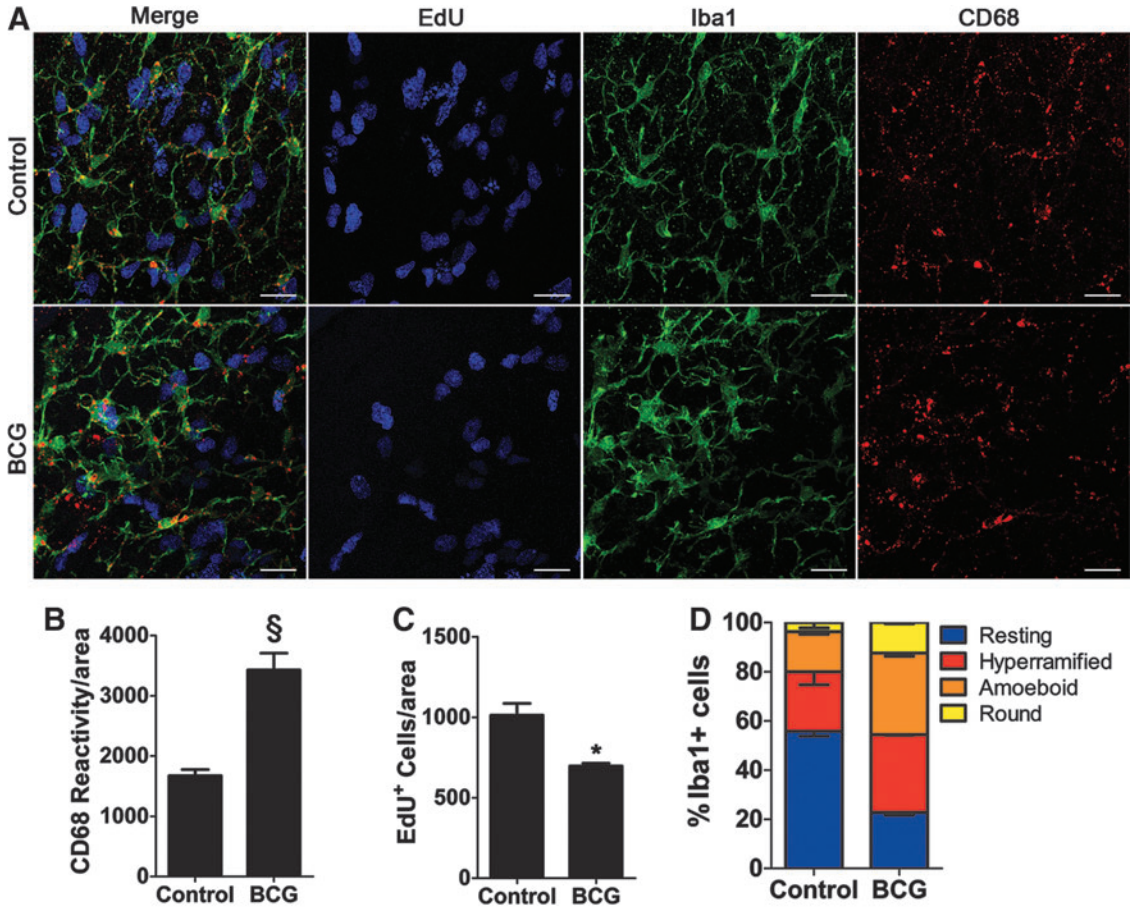

FIG. 6. Intraperitoneal inoculation with Bacillus Calmette–Guérin induces microglia activation and reduces neurogenesis in the V-SVZ. **(A)** Representative images of Iba1, EdU incorporation, and CD68 in V-SVZ wholemounts of mice 2 weeks after BCG inoculation or vehicle injected controls. Scale bar: 20 μm. **(B)** Quantification of CD68 immunoreactivity in the V-SVZ 2 weeks following inoculation with BCG. **(C)** Quantification of the number of EdU-positive cells in the V-SVZ in mice inoculated with BCG or vehicle. $n = 3$ per group. $^{*}P \leq 0.05$; $^{\S}P \leq 0.01$. **(D)** Quantification of the different stages of microglia activation (as in Fig. 4**A–D**) in the V-SVZ wholemounts after 2 weeks of BCG inoculation ($n = 3$ per group). Error bars = SEM.

compared to NSCs cultured in M0 conditioned medium (Fig. 7A, C; 35.05% ± 1.855% vs. 0.96% ± 0.4822% βIII-tubulin-positive cells per field; $P = 0.0003$), whereas M0 conditioned media induced a significant increase in neuron production when compared to controls (Fig. 7A, C; 35.05% ± 1.855% vs. 17.20% ± 2.947% βIII-tubulin-positive cells per field; $P = 0.0003$). All this indicates that microglia activation has a significant influence on NSC proliferation and neurogenesis.

Discussion

Adult neurogenesis continues in two distinct regions of the brain, the dentate gyrus of the hippocampus and the V-SVZ lining the lateral ventricle. The microenvironment or niche is a complex heterogeneous population of cells consisting of progenitors, endothelial cells, ependymal cells, and glia. Although, work by others has identified microglia as pro-neurogenic in the early postnatal period [38,50–52], very little is known about the role of microglia in the adult and aging V-SVZ niche. Using a V-SVZ wholemounts system that preserves the 3-dimensional relationship of cells within the niche, we characterized the spatiotemporal changes and activation state of microglia in the young adult and aged V-SVZ.

We found that microglia in young adult mice (2 months old) were distributed uniformly throughout the V-SVZ and were closely associated with NSC germinal pinwheels, transit-amplifying cells, neuroblasts, GFAP-positive niche cells, and the vascular plexus. Thus, microglia are positioned to influence NSCs and their progeny as well as other niche cells known to be important in regulating NSC behavior. By mid-age (12 months), microglia's uniformity within the V-SVZ niche deteriorated and observed a trend of increase of clusters of activated microglia between 2, 6, and 12 months, reaching significance by 24 months. We measured a distinct shift in the distribution of microglia in the V-SVZ observing hyper-ramified intermediate activated microglia increasing in association with germinal pinwheels and ependymal cells.

In contrast, microglia associated with the vasculature retracted their processes, became more amoeboid, and were located farther away from the niche vasculature during aging. Microglia play a key role in angiogenesis during development, and depletion of retinal microglia results in reduced vascular density [53]. Vascular density is reduced in

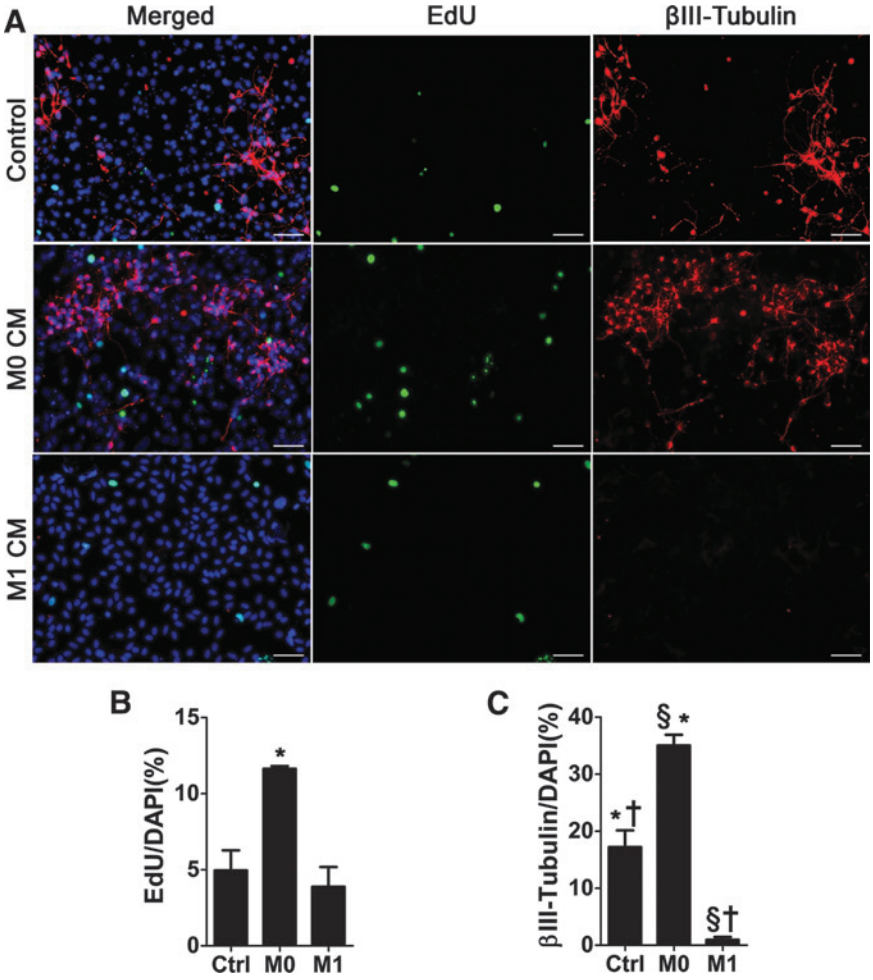

FIG. 7. Activated microglia reduces neurogenesis, whereas resting microglia increases proliferation and neurogenesis in vitro. **(A)** Representative images of NSC cultures treated with conditioned medium from activated microglia (M1), resting microglia (M0), or control medium from NSCs. Scale bar: 50 μm. **(B)** Quantification of EdU-positive nuclei per DAPI in control, M0, and M1 CM-treated NSC cultures ($*P \leq 0.05$). **(C)** Percentage of β-Tubulin-positive cells in relation to DAPI ($*/^{\dagger}P \leq 0.01$; $^{\S}P \leq 0.001$). Error bars = SEM. $n = 3$ per group.

the aging V-SVZ [23], which likely contributes to NSC dysfunction. Little is known about the role of microglia in vascular remodeling in the adult V-SVZ, however, microglia accumulation has been shown to precede vascular recruitment and remodeling in the V-SVZ following EGF infusion into the lateral ventricle [54] suggesting that the reduced association of microglia and the vasculature we see during aging could contribute to age-associated changes in the vascular niche.

We observed increased activation of microglia during aging based on morphology and increased expression of Iba1 and CD68. Strikingly, evidence for inflammation was seen in the adult V-SVZ in mice as young as 6 months of age based on increased CD68 reactivity and IL-6 expression compared to 2-month-old adult mice. This increase in inflammatory markers occurred before the reduction in V-SVZ neurogenesis was observed between 6 and 12 months of age. This early and sustained microglia activation was unique to the adult V-SVZ as we did not observe overt activation of microglia in the striatum or cortex until 24 months of age, suggesting that microglia in the V-SVZ NSC niche are specialized and sustained activation of microglia likely contributes to reduced neurogenesis at mid-age.

The degree of activation of V-SVZ microglia could be due to exposure to proinflammatory factors in the cerebrospinal fluid (CSF). We found that a subpopulation of microglia associated with germinal pinwheels send processes through the ependymal layer making direct contact with CSF in the lateral ventricle. Another possibility is that microglia in this region are in greater demand as phagocytes because of increasing cell turnover in the aging SVZ. This has also been described in the young adult dentate gyrus, where microglia clear newborn neurons undergoing apoptosis when they fail to integrate into the existing circuitry [36]. However, apoptosis is rare [43,55] and microglia are not phagocytic [56] in the young adult V-SVZ. Therefore, whether there is an increase in cell turnover and apoptosis in the aged V-SVZ, and if microglia are involved remains an interesting topic to be investigated.

Microglia number increased in the V-SVZ during aging and we investigated if this was, at least in part, due to peripheral monocytes infiltrating into the niche. In this study we used transgenic mice that express GFP under the Cx3cr1 promoter and RFP under the CCr2 promoter. These mice have been shown to be a valuable tool to distinguish resident microglia from peripheral monocytes based on RFP expression [25]. We saw a significant increase in the number of cells that express RFP in a punctate pattern within GFP-expressing cells. We interpreted these as infiltrating peripheral monocytes, however, we did not rule out the possibility that these were instead peripheral RFP+ monocytes that had been phagocytosed by resident microglia. Either interpretation suggests that there is significant infiltration of peripheral monocytes into the neurogenic niche during aging and it will

be important in future studies to determine if these infiltrating cells have a unique influence on neurogenesis and the surrounding niche. In hippocampal neurogenesis, cross-talk between infiltrating T cells and resident microglia in the hippocampus has been demonstrated to be crucial in mediating the proneurogenic effects of environmental enrichment in mice [37].

We also observed an increase in proinflammatory cytokines in the V-SVZ between young adult and aged mice, indicative of a pronounced switch to a proinflammatory extracellular environment within the neurogenic niche. Inflammatory cytokines can have profound effects on NSC function and likely contribute directly to reduced neurogenesis in the aging brain. We have previously found that in young adult mice, IL-1β increases VCAM1 expression on NSCs within germinal pinwheels, maintaining them in a quiescent state, hampering lineage progression, and diminishing the transient-amplifying pool [20]. Of note, we observed remodeling of VCAM1 on germinal pinwheels during aging. Thus, the reductions we observed in neurogenesis in the aging brain could reflect an increase in NSC quiescence and lack of lineage progression. This is supported by findings of reduced EGFR expression and signaling in aged mice [18], a hallmark of NSC activation [57,58].

Microglia signals likely work with other niche molecules known to influence NSC behavior such as those from the vasculature [42,43,59–61], CSF [20,62,63], and ependymal cells [64]. Numerous reports suggest that activation of microglia can be proneurogenic or antineurogenic in the V-SVZ depending on the context. During cortical development, microglia display an amoeboid morphology in the embryonic brain and limit cortical neurogenesis through phagocytosis of neural progenitors [65]. Amoeboid microglia accumulate in the V-SVZ during the early postnatal period (P1-10) and are proneurogenic [38,50,52] through the secretion of IL-1β, IL-6, TNF-α, and IFN-γ. These amoeboid microglia then transition to a resting ramified morphology by postnatal day 30 [38].

Likewise, NSC proliferation is increased in many animal models of brain pathology associated with microglia activation and brain inflammation such as ischemia [66], traumatic brain injury [67], and multiple sclerosis [33], and this is thought to be important in the endogenous repair response. However, in conditions such as allergic encephalomyelitis [68] and status epilepticus [69,70] neurogenesis is suppressed. The activation state of microglia in each of these different conditions likely alters the concentrations and combinations of cytokines released, which results in either increased or decreased neurogenesis. In support of this, coculture studies in which NSCs are cultured with proneurogenic early postnatal microglia show that blockade of IL-1β, IFN-γ, IL-6, and TNFα reduces neurogenesis, but inhibition of any of these cytokines singly had no effect, suggesting that these cytokines act in combination during early postnatal neurogenesis [38]. In addition, NSC cultures in the presence of low concentration (1 ng/mL) TNFα exhibit increased proliferation, whereas high concentrations (10–100 ng/mL) TNFα causes apoptosis [71]. Thus, it is likely that the early and sustained activation of microglia we observed in the aging V-SVZ results in a cytokine milieu and concentration that is not supportive of long-term neurogenesis either by acting directly on NSCs and/or by acting on other niche cells.

Using a coculture system revealed that secreted factors from resting microglia increase NSC proliferation and neuronal output compared to nonconditioned medium, which suggests that microglia under homeostatic conditions are supportive of neurogenesis. However, there is very little understanding of the activation state or what role microglia play in neurogenesis in the adult V-SVZ after the postnatal period. Microglia are denser in neurogenic regions compared to non-neurogenic regions and are much more proliferative [50,72]. Although microglia in the V-SVZ have a ramified resting morphology they express higher levels of CD45 and IB4 than microglia in the cortex [50] suggesting they are specialized in this region.

More study is needed to understand the role of microglia in regulating adult neurogenesis during tissue homeostasis and pathological conditions. Given that microglia are antineurogenic during cortical development [65], proneurogenic during the early postnatal period [38], and inhibit neurogenesis in the context of aging, microglia likely play different roles in neurogenesis depending on the developmental stage, inflammatory stimuli, and activation state.

Acknowledgments

This work received computational support from Computational System Biology Core, funded by the National Institute on Minority Health and Health Disparities (G12MD 007591) from the National Institutes of Health. Images were generated in the Core Optical Imaging Facility, which is supported by UTHSCSA, NIH-NCI P30 CA54174 (CTRC at UTHSCSA) and NIH-NIA P01AG19316. Data were generated in the Flow Cytometry Shared Resource Facility, which is supported by UTHSCSA, NIH-NCI P30 CA 054174-20 (CTRC at UTHSCSA), and UL1 TR001120 (CTSA grant). This work was supported in part by the William and Ella Owens Medical Research Foundation and Nathan Shock Center of Excellence in Basic Biology of Aging to EK and by the National Institutes of Health grant SC1GM095426 to AEC.

Disclosure statement

No competing financial interests exist.

References

1. Alvarez-Buylla A, JM Garcia-Verdugo and AD Tramontin. (2001). A unified hypothesis on the lineage of neural stem cells. Nat Rev Neurosci 2:287–293.
2. Doetsch F and A Alvarez-Buylla. (1996). Network of tangential pathways for neuronal migration in adult mammalian brain. Proc Natl Acad Sci U S A 93:14895–14900.
3. Eriksson PS, E Perfilieva, T Bjork-Eriksson, AM Alborn, C Nordborg, DA Peterson and FH Gage. (1998). Neurogenesis in the adult human hippocampus. Nat Med 4:1313–1317.
4. Seri B, JM Garcia-Verdugo, BS McEwen and A Alvarez-Buylla. (2001). Astrocytes give rise to new neurons in the adult mammalian hippocampus. J Neurosci 21:7153–7160.
5. Gage FH, G Kempermann, TD Palmer, DA Peterson and J Ray. (1998). Multipotent progenitor cells in the adult dentate gyrus. J Neurobiol 36:249–266.
6. van Praag H, AF Schinder, BR Christie, N Toni, TD Palmer and FH Gage. (2002). Functional neurogenesis in the adult hippocampus. Nature 415:1030–1034.

7. Miller JA, J Nathanson, D Franjic, S Shim, RA Dalley, S Shapouri, KA Smith, SM Sunkin, A Bernard, et al. (2013). Conserved molecular signatures of neurogenesis in the hippocampal subgranular zone of rodents and primates. Development 140:4633–4644.
8. Zhao C, EM Teng, RG Summers, Jr, GL Ming and FH Gage. (2006). Distinct morphological stages of dentate granule neuron maturation in the adult mouse hippocampus. J Neurosci 26:3–11.
9. Seri B, JM Garcia-Verdugo, L Collado-Morente, BS McEwen and A Alvarez-Buylla. (2004). Cell types, lineage, and architecture of the germinal zone in the adult dentate gyrus. J Comp Neurol 478:359–378.
10. Lois C and A Alvarez-Buylla. (1994). Long-distance neuronal migration in the adult mammalian brain. Science 264:1145–1148.
11. Arvidsson A, T Collin, D Kirik, Z Kokaia and O Lindvall. (2002). Neuronal replacement from endogenous precursors in the adult brain after stroke. Nat Med 8:963–970.
12. Holmin S, P Almqvist, U Lendahl and T Mathiesen. (1997). Adult nestin-expressing subependymal cells differentiate to astrocytes in response to brain injury. Eur J Neurosci 9: 65–75.
13. Nait-Oumesmar B, L Decker, F Lachapelle, V Avellana-Adalid, C Bachelin and A Baron-Van Evercooren. (1999). Progenitor cells of the adult mouse subventricular zone proliferate, migrate and differentiate into oligodendrocytes after demyelination. Eur J Neurosci 11:4357–4366.
14. Tattersfield AS, RJ Croon, YW Liu, AP Kells, RL Faull and B Connor. (2004). Neurogenesis in the striatum of the quinolinic acid lesion model of Huntington's disease. Neuroscience 127:319–332.
15. Thored P, A Arvidsson, E Cacci, H Ahlenius, T Kallur, V Darsalia, CT Ekdahl, Z Kokaia and O Lindvall. (2006). Persistent production of neurons from adult brain stem cells during recovery after stroke. Stem Cells 24:739–747.
16. Shook BA, DH Manz, JJ Peters, S Kang and JC Conover. (2012). Spatiotemporal changes to the subventricular zone stem cell pool through aging. J Neurosci 32:6947–6956.
17. Bouab M, GN Paliouras, A Aumont, K Forest-Berard and KJ Fernandes. (2011). Aging of the subventricular zone neural stem cell niche: evidence for quiescence-associated changes between early and mid-adulthood. Neuroscience 173:135–149.
18. Tropepe V, CG Craig, CM Morshead and D van der Kooy. (1997). Transforming growth factor-alpha null and senescent mice show decreased neural progenitor cell proliferation in the forebrain subependyma. J Neurosci 17: 7850–7859.
19. Enwere E, T Shingo, C Gregg, H Fujikawa, S Ohta and S Weiss. (2004). Aging results in reduced epidermal growth factor receptor signaling, diminished olfactory neurogenesis, and deficits in fine olfactory discrimination. J Neurosci 24:8354–8365.
20. Kokovay E, Y Wang, G Kusek, R Wurster, P Lederman, N Lowry, Q Shen and S Temple. (2012). VCAM1 is essential to maintain the structure of the SVZ niche and acts as an environmental sensor to regulate SVZ lineage progression. Cell Stem Cell 11:220–230.
21. Conover JC and BA Shook. (2011). Aging of the subventricular zone neural stem cell niche. Aging Dis 2:49–63.
22. Mirzadeh Z, FT Merkle, M Soriano-Navarro, JM Garcia-Verdugo and A Alvarez-Buylla. (2008). Neural stem cells confer unique pinwheel architecture to the ventricular surface in neurogenic regions of the adult brain. Cell Stem Cell 3: 265–278.
23. Katsimpardi L, NK Litterman, PA Schein, CM Miller, FS Loffredo, GR Wojtkiewicz, JW Chen, RT Lee, AJ Wagers and LL Rubin. (2014). Vascular and neurogenic rejuvenation of the aging mouse brain by young systemic factors. Science 344:630–634.
24. Luo J, SB Daniels, JB Lennington, RQ Notti and JC Conover. (2006). The aging neurogenic subventricular zone. Aging Cell 5:139–152.
25. Mizutani M, PA Pino, N Saederup, IF Charo, RM Ransohoff and AE Cardona. (2012). The fractalkine receptor but not CCR2 is present on microglia from embryonic development throughout adulthood. J Immunol 188: 29–36.
26. Butovsky O, MP Jedrychowski, CS Moore, R Cialic, AJ Lanser, G Gabriely, T Koeglsperger, B Dake, PM Wu, et al. (2014). Identification of a unique TGF-β-dependent molecular and functional signature in microglia. Nat Neurosci 17:131–143.
27. Nimmerjahn A, F Kirchhoff and F Helmchen. (2005). Resting microglial cells are highly dynamic surveillants of brain parenchyma in vivo. Science 308:1314–1318.
28. Banati RB, J Gehrmann, P Schubert and GW Kreutzberg. (1993). Cytotoxicity of microglia. Glia 7:111–118.
29. Colton CA and DL Gilbert. (1987). Production of superoxide anions by a CNS macrophage, the microglia. FEBS Lett 223:284–288.
30. Hefendehl JK, JJ Neher, RB Suhs, S Kohsaka, A Skodras and M Jucker. (2014). Homeostatic and injury-induced microglia behavior in the aging brain. Aging Cell 13: 60–69.
31. Wong WT. (2013). Microglial aging in the healthy CNS: phenotypes, drivers, and rejuvenation. Front Cell Neurosci 7:22.
32. Lucin KM and T Wyss-Coray. (2009). Immune activation in brain aging and neurodegeneration: too much or too little? Neuron 64:110–122.
33. Butovsky O, G Landa, G Kunis, Y Ziv, H Avidan, N Greenberg, A Schwartz, I Smirnov, A Pollack, S Jung and M Schwartz. (2006). Induction and blockage of oligodendrogenesis by differently activated microglia in an animal model of multiple sclerosis. J Clin Invest 116:905–915.
34. Ekdahl CT, JH Claasen, S Bonde, Z Kokaia and O Lindvall. (2003). Inflammation is detrimental for neurogenesis in adult brain. Proc Natl Acad Sci U S A 100: 13632–13637.
35. Monje ML, H Toda and TD Palmer. (2003). Inflammatory blockade restores adult hippocampal neurogenesis. Science 302:1760–1765.
36. Sierra A, JM Encinas, JJP Deudero, JH Chancey, G Enikolopov, LS Overstreet-Wadiche, SE Tsirka and M Maletic-Savatic. (2010). Microglia shape adult hippocampal neurogenesis through apoptosis-coupled phagocytosis. Cell Stem Cell 7:483–495.
37. Ziv Y, N Ron, O Butovsky, G Landa, E Sudai, N Greenberg, H Cohen, J Kipnis and M Schwartz. (2006). Immune cells contribute to the maintenance of neurogenesis and spatial learning abilities in adulthood. Nat Neurosci 9: 268–275.
38. Shigemoto-Mogami Y, K Hoshikawa, JE Goldman, Y Sekino and K Sato. (2014). Microglia enhance neurogenesis and oligodendrogenesis in the early postnatal subventricular zone. J Neurosci 34:2231–2243.

39. Livak KJ and TD Schmittgen. (2001). Analysis of relative gene expression data using real-time quantitative PCR and the 2(-Delta Delta C(T)) method. Methods 25: 402–408.
40. O'Connor JC, MA Lawson, C André, EM Briley, SS Szegedi, J Lestage, N Castanon, M Herkenham, R Dantzer and KW Kelley. (2009). Induction of IDO by bacille calmette-guérin is responsible for development of murine depressive-like behavior. J Immunol 182:3202–3212.
41. Durafourt BA, CS Moore, DA Zammit, TA Johnson, F Zaguia, M-C Guiot, A Bar-Or and JP Antel. (2012). Comparison of polarization properties of human adult microglia and blood-derived macrophages. Glia 60:717–727.
42. Kokovay E, S Goderie, Y Wang, S Lotz, G Lin, Y Sun, B Roysam, Q Shen and S Temple. (2010). Adult SVZ lineage cells home to and leave the vascular niche via differential responses to SDF1/CXCR4 signaling. Cell Stem Cell 7: 163–173.
43. Shen Q, Y Wang, E Kokovay, G Lin, SM Chuang, SK Goderie, B Roysam and S Temple. (2008). Adult SVZ stem cells lie in a vascular niche: a quantitative analysis of niche cell-cell interactions. Cell Stem Cell 3:289–300.
44. Palmer TD, AR Willhoite and FH Gage. (2000). Vascular niche for adult hippocampal neurogenesis. J Comp Neurol 425:479–494.
45. Streit WJ, SA Walter and NA Pennell. (1999). Reactive microgliosis. Prog Neurobiol 57:563–581.
46. Le Belle JE, NM Orozco, AA Paucar, JP Saxe, J Mottahedeh, AD Pyle, H Wu and HI Kornblum. (2011). Proliferative neural stem cells have high endogenous ROS levels that regulate self-renewal and neurogenesis in a PI3K/Akt-dependant manner. Cell Stem Cell 8:59–71.
47. Moreau M, J Lestage, D Verrier, C Mormede, KW Kelley, R Dantzer and N Castanon. (2005). Bacille calmette-guerin inoculation induces chronic activation of peripheral and brain indoleamine 2,3-dioxygenase in mice. J Infect Dis 192:537–544.
48. Drude S, A Geissler, J Olfe, A Starke, G Domanska, C Schuett and C Kiank-Nussbaum. (2011). Side effects of control treatment can conceal experimental data when studying stress responses to injection and psychological stress in mice. Lab Anim (NY) 40:119–128.
49. Nair A and RH Bonneau. (2006). Stress-induced elevation of glucocorticoids increases microglia proliferation through NMDA receptor activation. J Neuroimmunol 171: 72–85.
50. Goings GE, DA Kozlowski and FG Szele. (2006). Differential activation of microglia in neurogenic versus non-neurogenic regions of the forebrain. Glia 54:329–342.
51. Marshall GP 2nd, LP Deleyrolle, BA Reynolds, DA Steindler and ED Laywell. (2014). Microglia from neurogenic and non-neurogenic regions display differential proliferative potential and neuroblast support. Front Cell Neurosci 8:180.
52. Walton NM, BM Sutter, ED Laywell, LH Levkoff, SM Kearns, GP Marshall, B Scheffler and DA Steindler. (2006). Microglia instruct subventricular zone neurogenesis. Glia 54:815–825.
53. Checchin D, F Sennlaub, E Levavasseur, M Leduc and S Chemtob. (2006). Potential role of microglia in retinal blood vessel formation. Invest Ophthalmol Vis Sci 47: 3595–3602.
54. Lindberg OR, A Brederlau and HG Kuhn. (2014). Epidermal growth factor treatment of the adult brain subventricular zone leads to focal microglia/macrophage accumulation and angiogenesis. Stem Cell Reports 2:440–448.
55. He XJ, H Nakayama, M Dong, H Yamauchi, M Ueno, K Uetsuka and K Doi. (2006). Evidence of apoptosis in the subventricular zone and rostral migratory stream in the MPTP mouse model of Parkinson disease. J Neuropathol Exp Neurol 65:873–882.
56. Ribeiro Xavier AL, BT Kress, SA Goldman, JR Lacerda de Menezes and M Nedergaard. (2015). A distinct population of microglia supports adult neurogenesis in the subventricular Zone. J Neurosci 35:11848–11861.
57. Codega P, V Silva-Vargas, A Paul, AR Maldonado-Soto, AM Deleo, E Pastrana and F Doetsch. (2014). Prospective identification and purification of quiescent adult neural stem cells from their in vivo niche. Neuron 82: 545–559.
58. Doetsch F, L Petreanu, I Caille, JM Garcia-Verdugo and A Alvarez-Buylla. (2002). EGF converts transit-amplifying neurogenic precursors in the adult brain into multipotent stem cells. Neuron 36:1021–1034.
59. Delgado AC, SR Ferron, D Vicente, E Porlan, A Perez-Villalba, CM Trujillo, P D'Ocon and I Farinas. (2014). Endothelial NT-3 delivered by vasculature and CSF promotes quiescence of subependymal neural stem cells through nitric oxide induction. Neuron 83:572–585.
60. Tavazoie M, L Van der Veken, V Silva-Vargas, M Louissaint, L Colonna, B Zaidi, JM Garcia-Verdugo and F Doetsch. (2008). A specialized vascular niche for adult neural stem cells. Cell Stem Cell 3:279–288.
61. Nakagomi T, A Nakano-Doi, M Kawamura and T Matsuyama. (2015). Do vascular pericytes contribute to neurovasculogenesis in the central nervous system as multipotent vascular stem cells? Stem Cells Dev 24:1730–1739.
62. Sawamoto K, H Wichterle, O Gonzalez-Perez, JA Cholfin, M Yamada, N Spassky, NS Murcia, JM Garcia-Verdugo, O Marin, et al. (2006). New neurons follow the flow of cerebrospinal fluid in the adult brain. Science 311:629–632.
63. Bifari F, I Decimo, C Chiamulera, E Bersan, G Malpeli, J Johansson, V Lisi, B Bonetti, G Fumagalli, G Pizzolo and M Krampera. (2009). Novel stem/progenitor cells with neuronal differentiation potential reside in the leptomeningeal niche. J Cell Mol Med 13:3195–3208.
64. Lim DA, AD Tramontin, JM Trevejo, DG Herrera, JM Garcia-Verdugo and A Alvarez-Buylla. (2000). Noggin antagonizes BMP signaling to create a niche for adult neurogenesis. Neuron 28:713–726.
65. Cunningham CL, V Martínez-Cerdeño and SC Noctor. (2013). Microglia regulate the number of neural precursor cells in the developing cerebral cortex. J Neurosci 33:4216–4233.
66. Thored P, U Heldmann, W Gomes-Leal, R Gisler, V Darsalia, J Taneera, JM Nygren, S-EW Jacobsen, CT Ekdahl, Z Kokaia and O Lindvall. (2009). Long-term accumulation of microglia with proneurogenic phenotype concomitant with persistent neurogenesis in adult subventricular zone after stroke. Glia 57:835–849.
67. Chirumamilla S, D Sun, MR Bullock and RJ Colello. (2002). Traumatic brain injury induced cell proliferation in the adult mammalian central nervous system. J Neurotrauma 19:693–703.
68. Ben-Hur T, O Einstein, R Mizrachi-Kol, O Ben-Menachem, E Reinhartz, D Karussis and O Abramsky. (2003). Transplanted multipotential neural precursor cells

migrate into the inflamed white matter in response to experimental autoimmune encephalomyelitis. Glia 41:73–80.
69. Iosif RE, CT Ekdahl, H Ahlenius, CJ Pronk, S Bonde, Z Kokaia, SE Jacobsen and O Lindvall. (2006). Tumor necrosis factor receptor 1 is a negative regulator of progenitor proliferation in adult hippocampal neurogenesis. J Neurosci 26:9703–9712.
70. Koo JW and RS Duman. (2008). IL-1beta is an essential mediator of the antineurogenic and anhedonic effects of stress. Proc Natl Acad Sci U S A 105:751–756.
71. Bernardino L, F Agasse, B Silva, R Ferreira, S Grade and JO Malva. (2008). Tumor necrosis factor-alpha modulates survival, proliferation, and neuronal differentiation in neonatal subventricular zone cell cultures. Stem Cells 26:2361–2371.
72. Mosher KI, RH Andres, T Fukuhara, G Bieri, M Hasegawa-Moriyama, Y He, R Guzman and T Wyss-Coray. (2012). Neural progenitor cells regulate microglia functions and activity. Nat Neurosci 15:1485–1487.

Address correspondence to:
Erzsebet Kokovay, PhD
Department of Cellular and Structural Biology
University of Texas Health Science Center at San Antonio
San Antonio, TX 78229

E-mail: kokovaye@uthscsa.edu

Received for publication October 2, 2015
Accepted after revision February 8, 2016
Prepublished on Liebert Instant Online February 9, 2016